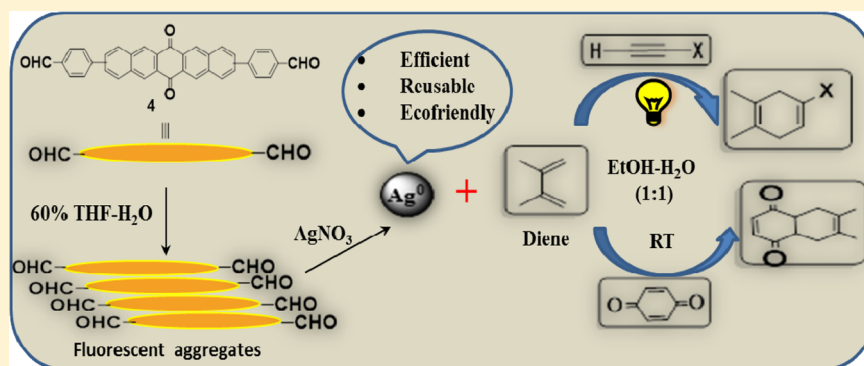


Pentacenequinone-Stabilized Silver Nanoparticles: A Reusable Catalyst for the Diels–Alder [4 + 2] Cycloaddition Reactions

Radhika Chopra, Kamaldeep Sharma, Manoj Kumar, and Vandana Bhalla*

Department of Chemistry, UGC Sponsored Centre for Advanced Studies-1, Guru Nanak Dev University, Amritsar, Punjab, India

S Supporting Information



ABSTRACT: Silver nanoparticles (AgNPs) stabilized by aggregates of derivative 4 have been used as catalyst for the construction of synthetically and biologically important [4 + 2] cycloadducts at room temperature.

INTRODUCTION

Among various organic transformations, Diels–Alder (DA) cycloaddition reactions for carbon–carbon bond formation are ideal because of their 100% theoretical atom economy.¹ Diels–Alder cycloaddition reactions of electron rich dienes with electron deficient carbonyl compounds proceed well, but for electronically mismatched partners forcing conditions are required.^{2–4} Under conventional conditions, DA reactions require prolonged reaction time and heating at high temperature which makes these reactions eco-unfriendly. The quest for environmentally benign reaction conditions has stimulated considerable research interest to develop new catalytic systems to carry out DA reactions under environmentally mild conditions.^{5–7} Consequently, over the past few years, various aspects of DA reactions such as factors affecting rate of reaction and catalysts have been extensively studied, and a variety of catalytic systems have been developed. However, most of these catalytic systems suffer from many limitations such as high cost of catalyst, formation of side products, use of organic solvent, and prolonged reaction time using high loading of catalyst which actually decrease the economic and environmental advantages of the methodology.^{8–11} Recently, ruthenium complexes have been reported which harvest visible light to carry out DA cycloaddition reactions.^{12–14} Though this photocatalytic system contributes toward saving energy and minimizing the undesirable side products, utilization of costly and toxic ruthenium metal as a major component of heterogeneous hybrid catalytic system and use of toxic dichloromethane as solvent remain as big hurdles toward the development of greener and sustainable chemical industry.

Thus, development of an efficient catalytic system for carrying out DA cycloaddition reactions under mild and environmentally benign conditions is still a challenge.

Recently, silica-supported AgNPs have been reported as heterogeneous catalysts for the preparation of various DA cycloadducts under thermal conditions using dichloromethane (DCM) as solvent¹⁵ which, however, decreased the eco-friendly advantage of the catalyst. Silver is known for its plasmonic nature and size dependent catalytic properties.¹⁶ In this context, we were interested in the development of a silver-based photocatalytic system for DA reaction.

Our research work involves the development of supramolecular assemblies and their utilization as reactors and stabilizers for the preparation of different types of metal NPs which were then used as catalysts for carrying out various types of organic transformations.^{17–21} Very recently, we developed and utilized supramolecular aggregates of pentacenequinone derivative 1 for the preparation of AgNPs having size in the range of 20–25 nm (Figure 1). These AgNPs exhibited

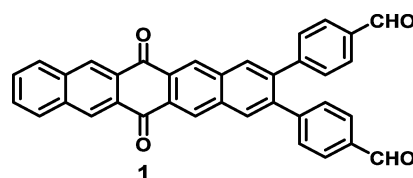
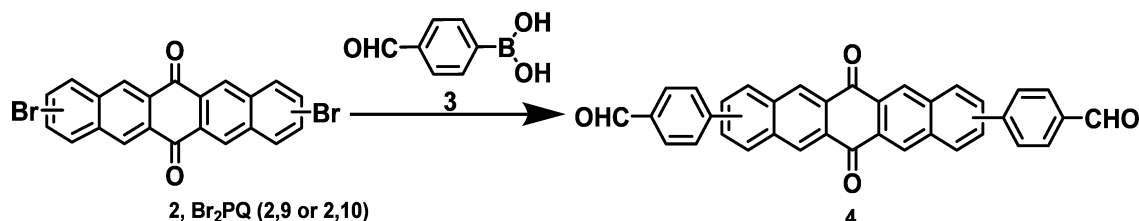


Figure 1. Structure of pentacenequinone derivative 1.

Received: November 10, 2015

Published: January 12, 2016

Scheme 1. Synthesis of Pentacenequinone-Based Derivative 4^a

^aConditions: Pd(0), K₂CO₃(aq), 1,4-dioxane.

moderate photocatalytic efficiency in degradation of rhodamine B under visible light illumination in the absence of any reducing agent or additive.²² In continuation of this work, we were then interested in the development of an efficient AgNPs based photocatalytic system for carrying out DA reaction. Since small sized NPs are known to exhibit better catalytic efficiency,²³ in the present investigation, we designed and synthesized pentacenequinone derivative 4 having 4-formylphenyl groups at 2,9 or 2,10 positions. We envisioned that the presence of aldehyde groups at pentacenequinone derivative 4 will assist the molecule to form a uniform layer around the silver ions during the reduction process; hence, growth of NPs will be restricted and thus will result in formation of AgNPs of smaller size. Interestingly, derivative 4 formed fluorescent aggregates in aqueous media due to its AIEE characteristics, and these aggregates exhibited strong affinity toward Ag⁺ ions and served as reactors and stabilizers for the preparation of AgNPs of average size of 7 nm. Furthermore, in situ generated AgNPs served as efficient photocatalyst for DA reactions between diene and alkynes in the absence of any additive or Lewis acid in aqueous media. Further, the DA cycloaddition reactions of activated systems such as quinone derivatives in the presence of derivative 4 stabilized AgNPs were complete in much shorter time to furnish the target molecules in excellent yields at room temperature. The photocatalytic/catalytic performance of in situ generated AgNPs is found to be better than the other systems reported in the literature (Table S1–S2, Supporting Information).

RESULTS AND DISCUSSION

Suzuki–Miyaura coupling of dibromopentacenequinone 2²⁴ [Br₂PQ (2,9 or 2,10)] with 4-formylphenylboronic acid 3 afforded derivative 4 in 61% yield (Scheme 1). The structure of derivative 4 was confirmed from its spectroscopic and analytical data (PSS2–S54, Supporting Information).

The ¹H NMR spectrum of derivative 4 showed four doublets (4H, 2H, 4H, and 2H) at 7.95, 8.01, 8.07, and 8.27 ppm corresponding to aromatic protons and four singlets (2H each) at 8.39, 9.02, 9.06, and 10.13 ppm corresponding to aromatic and aldehydic protons. The mass spectrum of derivative 4 showed a parent ion peak at *m/z* 517.1299 (M + H)⁺. The FT-IR spectrum of derivative 4 showed absorption peaks at 1701 and 1674 cm⁻¹ corresponding to carbonyl groups of aldehydic and ketonic moieties, respectively. The distinct peaks in the region of 1455–1616 cm⁻¹ correspond to the stretching vibrations of C=C double bonds of aromatic rings of derivative 4. Further, the absorbance peaks at 2840 and 3051 cm⁻¹ correspond to –CH₂ and =CH stretching vibrations, respectively. These spectroscopic data corroborate the structure 4 for this compound.

The UV–vis spectrum of derivative 4 in THF exhibits two absorption bands at 318 and 422 nm, respectively (Figure S1, Supporting Information). Upon addition of water (60%, v/v) to the THF solution of derivative 4, the absorbance of the entire spectrum gradually increased with the appearance of a level-off tail in the visible region (Figure S2, Supporting Information), which suggests the formation of aggregates. The solution of derivative 4 in THF is weakly emissive when excited at 318 nm (Φ_f = 0.01). Upon addition of water fraction up to 60%, an increase in emission intensity is observed at 493 nm (Φ_f = 0.34). Upon increase in water fraction up to 90%, a decrease in emission intensity was observed (Figure S3, Supporting Information). Usually compounds with AIEE characteristics show this phenomenon as after the aggregation only the molecules on the surface of the aggregates emit light and contribute to the fluorescence intensity upon excitation.^{25–28} The viscosity dependent fluorescence studies of derivative 4 in DMSO/glycerol were carried out to verify the AIEE phenomena (Figure S4, Supporting Information). As expected, the solution of derivative 4 becomes more emissive with increase in fraction of glycerol. Further, time-resolved fluorescence studies of derivative 4 in H₂O–THF (6:4) mixture show a large decrease in the nonradiative decay constant (K_{nr}) from 6.61 × 10⁹ s⁻¹ to 1.42 × 10⁹ s⁻¹ (Figure S5 and Table S3, Supporting Information). On the basis of viscosity dependent studies and time-resolved fluorescence studies, we believe that restriction to intramolecular motion is the main reason for AIEE phenomenon. The transmission electron microscopy (TEM) images of derivative 4 in H₂O–THF (6:4) solvent mixture show the presence of irregular-shaped aggregates (Figure S6, Supporting Information). The dynamic light scattering (DLS) analysis of derivative 4 in H₂O–THF (6:4) mixture indicates average size of aggregates in the range of 91–122 nm (Figure S7, Supporting Information). The presence of aldehyde groups prompted us to evaluate the binding behavior of aggregates of derivative 4 toward different metal ions such as Ag⁺, Al³⁺, Ba²⁺, Ca²⁺, Pd²⁺, Cd²⁺, Co²⁺, Cu²⁺, Fe³⁺, Fe²⁺, Hg²⁺, K⁺, Li⁺, Mg²⁺, Na⁺, Ni²⁺, Pb²⁺, and Zn²⁺ as their perchlorate/chloride/nitrate salt using UV–vis and fluorescence spectroscopy (Figures S8–S11, Supporting Information). However, no significant change was observed with these metal ions except Ag⁺ ions. Upon gradual addition of Ag⁺ ions (100 equiv) to the solution of derivative 4 in mixed aqueous media (H₂O–THF, 6:4), a characteristic surface plasmon resonance (SPR) band was observed at 454 nm in the UV–vis spectrum which suggests the formation of spherical AgNPs (Figure S12, Supporting Information). The intensity of this band increased with time, and the rate constant for the formation of AgNPs was found to be 1.08 × 10⁻⁴ s⁻¹ (Figure S13 and PS13, Supporting Information).^{29,30} On the other hand, complete quenching of fluorescence emission was observed upon

addition of Ag^+ ions (0–100 equiv) to the solution of derivative 4 (H_2O –THF, 6:4) (Figure S14, Supporting Information). This quenching in fluorescence emission is attributed to the binding of Ag^+ ions with nanoaggregates of derivative 4. The TEM image of aggregates of derivative 4 in the presence of Ag^+ ions shows the presence of spherical AgNPs having average size of 7 nm (Figure 2 and Figure S15, Supporting Information).

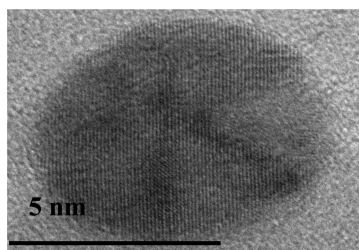


Figure 2. HRTEM image of spherical AgNPs of derivative 4; scale bar 5 nm.

The powder X-ray diffraction (XRD) studies of crystalline residue obtained after evaporation of solution of 4 and Ag^+ ions show the presence of diffraction peaks located at 2θ values of 29.46, 43.34, 70.36, 75.06, and 78.04, which suggests the formation of AgNPs (Figure S16, Supporting Information).³¹

To get insight into the mechanism of formation of AgNPs, the solution of aggregates of derivative 4 containing AgNPs was slowly evaporated. After several days, precipitates were observed which were filtered and washed with THF. After evaporation of THF, a residue was obtained whose ^1H NMR spectrum showed the upfield shift of aromatic signals, and a new peak was observed at 11.45 ppm corresponding to proton of carboxylic acid group (Figure S17, Supporting Information). The FTIR studies of the residue showed the presence of a new absorption band at 1776 cm^{-1} corresponding to carbonyl group of carboxylic acid (Figure S18, Supporting Information). We also carried out UV–vis studies of derivative 4 in the presence of Ag^+ ions in THF, but absorption spectra did not indicate any absorption band corresponding to AgNPs (Figure S19, Supporting Information). These studies highlight the role of aggregates of derivative 4 in preparation of AgNPs. On the basis of these results, we believe that upon addition of Ag^+ ions to the solution of aggregates of derivative 4, the Ag^+ ions interact with the aldehyde groups and get reduced to AgNPs. On the other hand, the aldehyde groups of aggregates of derivative 4 are oxidized to carboxylic acids which then stabilize AgNPs (Figure S20, Supporting Information).³² Thus, aggregates of derivative 4 having aldehyde groups serve as reactors for the generation of AgNPs, and the oxidized species of pentacenequinone derivative 4 having acidic groups serve as stabilizers for AgNPs.

In the next part of our work, we planned to examine the catalytic activity of in situ generated AgNPs in Diels–Alder (DA) cycloaddition reaction. To evaluate the effect of solvents, first, DA reaction of phenyl acetylene, 5a, with 2,3-dimethyl-1,3-butadiene, 6, was carried out in different solvents such as toluene, EtOH, DCM, and EtOH– H_2O (1:1) solvents at room temperature. The reaction did not proceed at room temperature in all the solvents except DCM (Table 1, entry 1). The desired product was obtained in lower yield upon heating the reaction mixture at high temperature for a longer period (24 h) in the presence of toluene and EtOH (Table 1, entries 3 and 5). The AgNPs are known to absorb the visible light,³³ and thus,

Table 1. Optimization of Reaction Conditions for AgNPs Catalyzed DA Reaction of Phenyl Acetylene, 5a, with 2,3-Dimethyl-1,3-butadiene, 6

| S. no. | reaction conditions | time (h) | yield |
|--------|---|----------|-------|
| 1 | DCM, RT | 4 | 70% |
| 2 | toluene, RT | 24 | – |
| 3 | toluene, 100 °C | 24 | 30% |
| 4 | EtOH, RT | 24 | – |
| 5 | EtOH, 80 °C | 20 | 45% |
| 6 | EtOH: H_2O (1:1), RT | 12 | – |
| 7 | EtOH: H_2O (1:1), visible light | 1.5 | 70% |

we planned to examine the catalytic efficiency of in situ generated AgNPs as photocatalysts in DA reaction. For this, we carried out the reaction of 5a and 6 in the presence of in situ generated AgNPs in EtOH– H_2O (1:1) solvent mixture under visible light irradiation. A 60 W tungsten filament bulb was used as the irradiation source, and the reaction vial was submerged in a water bath to prevent the photoheating effect. Interestingly, the reaction was complete in 1.5 h, and the desired product was obtained in 70% yield (Table 1, entry 7). This result suggests the possible application of derivative 4 stabilized AgNPs as a photocatalyst in DA reaction. To understand the influence of stabilizing agent on photocatalytic efficiency of AgNPs in the DA reaction, we carried out model reaction using pentacenequinone derivative 1 stabilized AgNPs. In presence of 0.07 mmol of pentacenequinone derivative 1 stabilized AgNPs, the reaction was complete in 4 h, and the desired product was obtained in 65% yield (Table 2, entry 1).

Table 2. Optimization of Reaction Conditions for AgNPs Catalyzed DA Reaction of Phenylacetylene, 5a, with 2,3-Dimethyl-1,3-butadiene, 6

| S. no. | catalyst | time (h) | yield |
|--------|-------------------------------|----------|-------|
| 1 | derivative 1 stabilized AgNPs | 4 | 65% |
| 2 | citrate-stabilized AgNPs | 7 | 63% |

Furthermore, we also carried out a model reaction in the presence of citrate-stabilized AgNPs prepared by the reported method.³⁴ The reaction was complete in 7 h, and the desired product was obtained in 63% yield (Table 2, entry 2). The above studies highlight the importance of catalytic efficiency of AgNPs stabilized by aggregates of pentacenequinone derivative 4.

We believe that higher catalytic activity of pentacenequinone derivative 4 stabilized AgNPs is due to their small size, large surface area, and spherical shape. In addition, aggregates of derivative 4 also play an important role in bringing the reactant molecules closer to catalytic sites, thus providing a facile synthetic route to prepare DA cycloadducts.

Thus, for carrying out further reaction, we choose 0.07 mmol of pentacenequinone derivative **4** stabilized AgNPs and EtOH–H₂O (1:1) as solvent mixture. To check the scope of substrates, we utilized the in situ generated AgNPs as catalyst in DA reactions of various dienophiles having electron-withdrawing or electron-donating groups (Table 3). All the reactions proceeded well, and desired products were obtained in good to excellent yields (PS26-S32, Supporting Information).

Table 3. AgNPs Catalyzed Photocatalytic DA Reaction of Various Alkynes with 2,3-Dimethyl-1,3-butadiene, **6**

| S. no. | X | yield |
|--------|---|-------|
| 1 | 5a/7a = –Ph | 70% |
| 2 | 5b/7b = –COOH | 83% |
| 3 | 5c/7c = –COOC ₂ H ₅ | 80% |
| 4 | 5d/7d = –CH ₂ OH | 64% |
| 5 | 5e/7e = –CH ₂ Br | 45% |

The substrates bearing electron-withdrawing groups furnished the desired products in excellent yields, and the reaction conditions tolerated the presence of hydroxyl and carboxylic

groups. Further, the efficiency of the in situ generated AgNPs was tested using various amounts of catalyst loading for the reaction between **5a** and **6**. With decrease in catalyst loading from 0.07 to 0.033 mmol, the product was formed in almost the same yield, but it took a longer time for completion (12 h). Such an extremely low quantity of catalyst has never been used successfully for DA reactions at room temperature before the present study. The same reactions when carried out in the absence of AgNPs furnished no product even after 24 h. To test the reusability of these NPs, the DA cyclization between **5a** and **6** was chosen as a model reaction. After completion of reaction, the reaction mixture containing catalyst was subjected to the next catalytic sequence by adding **5a** and **6** to the reaction mixture. The complete conversion of **5a** to DA cycloadduct occurs up to three cycles in the presence of derivative **4** stabilized AgNPs. Further, recyclability of AgNPs generated by aggregates of derivative **4** was checked for the same reaction. The oily product was extracted with pentane, and the aqueous layer containing AgNPs was reused at least three times using this recycling procedure for identical reactions (Figure S21, Supporting Information). The yield of desired product remained almost the same after three recycling reactions (respectively 70%, 67%, 65%). To get insight into the mechanism of photocatalytic DA reaction, we carried out DA reaction between **5a** and **6** in the presence of triethanolamine (TEOA) as hole scavenger, and the reaction was complete in 1.5 h to afford desired cycloadduct in 62% yield. We also

Table 4. DA Cyclization Strategy Involving Quinones as Dienophiles and 2,3-Dimethyl-1,3-butadiene, **6**, Utilizing Derivative **4** Stabilized AgNPs

| S.No. | Dienophile | Product | Time | Yield |
|-------|------------|---------|------|-------|
| 1. | | | 4 h | 84% |
| 2. | | | 7 h | 81% |
| 3. | | | 7 h | 80% |
| 4. | | | 10 h | 76% |
| 5. | | | 12 h | 73% |

carried out the same reaction in the presence of CuSO_4 as an electron scavenger, and the desired product was obtained in traces. These studies suggest that photogenerated electron pair is essential to carry out the DA reactions.

Further, we employed DA cyclization strategy using highly activated dienophiles such as pyran and maleic anhydride. Interestingly, in situ generated AgNPs exhibited good catalytic efficiency in these reactions. The reactions were complete in 3 h at room temperature to furnish pyran and maleic anhydride derivatives in good yield (PS33-S36 and Table S4, Supporting Information). Encouraged by excellent catalytic activity of derivative 4 stabilized AgNPs in DA reactions, we planned to utilize in situ generated AgNPs as catalyst for carrying out synthesis of various quinone derivatives. Quinone derivatives are oxidative intermediates of natural polyphenols and widely exist in medicinal plants or food. The conventional conditions require prolonged heating of the reaction mixture to get the desired products in good yields. However, in the presence of 0.07 mmol of AgNPs, the reaction between 2,3-dimethyl-1,3-butadiene, **6**, and *p*-benzoquinone, **8a**, was complete in 4 h.

Further, to widen the scope of reaction, various quinones (**8a–8e**) were subjected to the DA reaction with the diene **6** in the presence of in situ generated AgNPs at room temperature to furnish the desired products (**9a–9e**) in good yields (Table 4 and PS43-S51, Supporting Information). Interestingly, the target products were purified by simple recrystallization with EtOH without using any other purification technique.

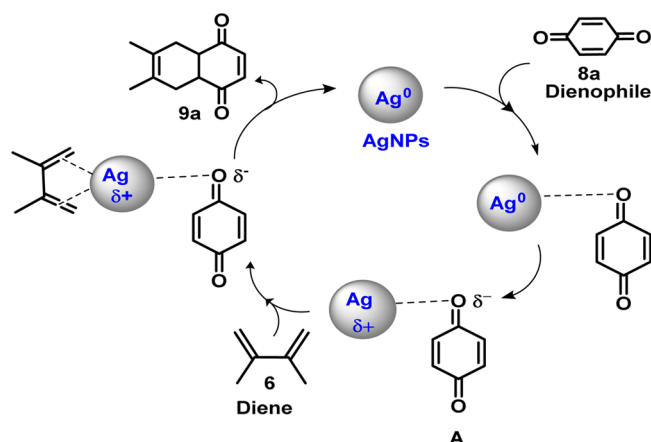
To get insight into the mechanism of the reaction, we selected the reaction between 2,3-dimethyl-1,3-butadiene, **6**, and *p*-benzoquinone, **8a**, as the model reaction. The UV–vis studies of reaction mixture of **6** and **8a** in EtOH– H_2O (1:1) in the absence of catalyst showed two absorption bands at 221 and at 440 nm corresponding to diene **6** and dienophile **8a**, respectively. Upon addition of AgNPs, the band at 440 nm is blue-shifted to 370 nm which suggests the interaction between the substrate **8a** and AgNPs. The absorption band at 370 nm may be assigned to the adduct **A** formed between AgNPs and substrate **8a**. After 4 h, a new band corresponding to product **9a** appeared at 305 nm (Figure S22, Supporting Information).

Furthermore, we investigated the kinetic studies of the reaction between **6** and **8a** in the presence of in situ generated AgNPs by UV–vis spectroscopy (Figures S23–S34, Supporting Information). These studies suggest that rate of reaction follows first-order kinetics with respect to diene **6**. In case of dienophile **8a**, rate of reaction follows first-order kinetics at low concentration (1 μM); however, saturation kinetics is observed at high concentration. We also carried out kinetic measurements of model reaction by using different concentrations of in situ generated AgNPs, and a linear relationship was observed between initial rate of reaction and concentration of in situ generated AgNPs. On the basis of these studies, a plausible reaction mechanism has been proposed for DA reaction between diene **6** and dienophile **8a** (Scheme 2). We propose that AgNPs interact with *p*-benzoquinone and get activated by acquiring a partial positive charge on their surface.³⁵ Further, the activated AgNPs bring diene and dienophile closer to each other which results in the formation of cycloadducts via concerted mechanism as shown in Scheme 2.

CONCLUSIONS

In summary, pentacenequinone derivative **4** having 4-formylphenyl groups at 2,9 or 2,10 positions has been designed and synthesized. Derivative **4** exhibits AIEE characteristics and

Scheme 2. Proposed Reaction Mechanism for DA Reaction Involving *p*-Benzoquinone as Dienophile



forms fluorescent aggregates in aqueous media. The aggregates of derivative **4** serve as reactors and stabilizers for the preparation of spherical AgNPs having size in the range of 7 nm which serve as an efficient and reusable photocatalysts/catalysts in the DA cycloaddition reactions.

EXPERIMENTAL SECTION

General Experimental Methods. Instruments. General experimental methods used in the present work were the same as reported earlier by us.³⁶ To record TEM images, transmission electron microscopy was used. IR spectrum (400–4000 cm^{-1}) was taken on an infrared (IR) spectrometer by using KBr pellets. Vibrational bands in IR spectra were reported as follows: frequency in cm^{-1} , intensity (*s* = sharp, *w* = weak). To perform elemental analysis (C, H, N), a CHNS-O analyzer was used. For carrying out photocatalytic experiments, a tungsten filament bulb (60 W) was used as irradiation source. FT-NMR (300 MHz) and FT-NMR (500 MHz) spectrophotometers were used to record ¹H NMR spectra. Coupling constants (*J*) and chemical shifts (δ) were expressed in Hz and ppm, respectively. Further, multiplicities of signals such as broad singlet, singlet, doublet, and multiplet were quoted as br s, s, d, and m, respectively.

Quantum yield calculations. To determine fluorescence quantum yield of derivative **4**, optically matching solution of diphenylanthracene ($\Phi_{\text{fr}} = 0.90$ in cyclohexane) was used as reference at an excitation wavelength (λ_{ex}) of 318 nm. In order to calculate quantum yield, the following equation was used:

$$\Phi_{\text{fs}} = \Phi_{\text{fr}} \times \frac{1 - 10^{-A_{\text{rLr}}}}{1 - 10^{-A_{\text{sLs}}}} \times \frac{N_{\text{s}}^2}{N_{\text{r}}^2} \times \frac{D_{\text{s}}}{D_{\text{r}}}$$

Φ_{fs} and Φ_{fr} are the fluorescence quantum yields of sample and reference, respectively. A_{s} , L_{s} , N_{s} , and D_{s} are the absorbance, length of the absorption cells, refractive index, and respective areas of emission of sample, respectively. A_{r} , L_{r} , N_{r} , and D_{r} are the absorbance, length of the absorption cells, refractive index, and respective areas of emission of reference, respectively.

Synthesis of 2,9 or 2,10-Bis(4-formylphenyl)-6,13-pentacenequinone, 4. To a mixture of compounds **2** (0.30 g, 1.56 mmol) and **3** (0.52 g, 3.44 mmol) in 20 mL of 1,4-dioxane was added 1 mL of aqueous solution of K_2CO_3 (1.72 g, 12.50 mmol) followed by addition of $[\text{Pd}(\text{PPh})_3]_4$ (0.35 g, 0.47 mmol) under N_2 atmosphere. The reaction mixture was

refluxed for 24 h. After completion of the reaction, the excess solvent was removed under reduced pressure, and the residue so obtained was dissolved in DCM. The organic layer was washed with water, dried over anhydrous Na_2SO_4 , and removed under reduced pressure to give a crude product which was purified by column chromatography using chloroform/hexane (80:20) as an eluent to afford derivative **4** (0.51 g in 61% yield); mp: >280 °C. ^1H NMR (500 MHz, CDCl_3 , ppm) δ = 7.95 (d, 4H, J = 7.5 Hz), 8.01 (d, 2H, J = 8.5 Hz), 8.07 (d, 4H, J = 7.5 Hz), 8.27 (d, 2H, J = 8 Hz), 8.39 (s, 2H), 9.02 (s, 2H), 9.06 (s, 2H), 10.13 (s, 2H); m/z = 517.1299 [$\text{M} + \text{H}$] $^+$; Elemental analysis: Calcd for $\text{C}_{36}\text{H}_{20}\text{O}_4$: C 83.71; H 3.90; O 12.39. Found: C 83.70; H 3.87; O 12.38. IR: (in cm^{-1}) 3051(w), 2840(w), 1701(s), 1674(s), 1616(s), 1603(s), 1582(s), 1455(s). The ^{13}C NMR spectrum of compound **4** could not be recorded due to its poor solubility.

Synthesis of AgNPs. A solution of compound **4** (10 μM , 3 mL) in $\text{H}_2\text{O}/\text{THF}$ (6/4, v/v) and AgNO_3 in water (0.1 M, 30 μL) was stirred for 4 h at room temperature. After 4 h, the color of the reaction mixture changed from colorless to greyish black which indicated the formation of AgNPs. These AgNPs were washed 4–5 times with distilled water to remove unreacted AgNO_3 and then were used as such for further catalytic application.

General Procedure for Synthesis of DA Cycloadducts (7a/7b/7c/7d/7e) Using in Situ Generated AgNPs. In a 25 mL round-bottom flask (RBF), terminal alkynes **5a/5b/5c/5d/5e** (0.1 g, 1.0 equiv) and 2,3-dimethyl-1,3-butadiene, **6** (4.0 equiv) were mixed in 10 mL of $\text{EtOH}:\text{H}_2\text{O}$ (1:1) solvent mixture in the presence of AgNPs (0.07 mmol). The reaction mixture was degassed under vacuum for 2–3 min and then irradiated with a 60 W tungsten filament bulb (0.24 W/cm^2) from a distance of 10 cm to provide visible light for 75 min. The reaction temperature was maintained at room temperature by putting RBF in a water bath. After completion of the reaction, excess EtOH was removed, and the remaining aqueous solution was extracted with pentane (2 \times 10 mL). The organic layer was dried over anhydrous Na_2SO_4 and distilled off to yield the desired product (7a/7b/7c/7d/7e). The aqueous layer containing AgNPs was then used as such for further catalytic reactions.

Compound 7a.³⁷ (4,5-Dimethylcyclohexa-1,4-dienyl)-benzene): (0.056 g in 70% yield). ^1H NMR (300 MHz, CDCl_3 , ppm) δ = 1.64 (s, 6H), 2.52–2.68 (m, 4H), 5.75 (t, 1H, J = 6.0 Hz), 7.43 (d, 2H, J = 6.0 Hz), 7.75–7.78 (m, 3H).

Compound 7b.³⁸ (4,5-Dimethylcyclohexa-1,4-dienecarboxylic acid): (0.180 g in 83% yield). ^1H NMR (300 MHz, CDCl_3 , ppm) δ = 1.67 (s, 3H), 1.70 (s, 3H), 2.87–2.88 (m, 4H), 7.08–7.10 (m, 1H).

Compound 7c.³⁹ (Ethyl 4,5-Dimethylcyclohexa-1,4-diene-carboxylate): (0.072 g in 80% yield). ^1H NMR (300 MHz, CDCl_3 , ppm) δ = 1.30 (t, 3H, J = 7.05 Hz), 1.65 (s, 3H), 1.68 (s, 3H), 2.82–2.83 (m, 4H), 4.21 (q, 2H, J = 7.05 Hz), 6.92–6.94 (m, 1H).

Compound 7d.³⁹ [(4,5-Dimethylcyclohexa-1,4-dienyl)-methanol]: (0.079 g in 64% yield). ^1H NMR (300 MHz, CDCl_3 , ppm) δ = 0.92 (br s, 1H), 1.52–1.62 (m, 6H), 2.36–2.42 (m, 2H), 2.52–2.58 (m, 2H), 3.76 (s, 2H), 5.50–5.56 (m, 1H).

Compound 7e. (4-Bromo-1,2-dimethylcyclohexa-1,4-diene): (Oily liquid, 0.038 g in 45% yield). ^1H NMR (300 MHz, CDCl_3 , ppm) δ = 1.63 (s, 3H), 1.68 (s, 3H), 2.37–2.39 (m, 2H), 2.48–2.50 (m, 2H), 3.66 (s, 2H), 5.86 (br s, 1H); ^{13}C

NMR (125 MHz, CDCl_3 , ppm) δ = 23.8, 28.9, 29.7, 38.8, 128.8, 130.9, 132.5; ESI-MS mass spectrum of compound **7e** showed a parent ion peak, m/z = 202.1938 [$\text{M} + \text{H}$] $^+$. Elemental analysis: Calcd for $\text{C}_9\text{H}_{13}\text{Br}$: C 53.75; H 6.52. Found: C 53.73; H 6.51.

General Procedure for Synthesis of DA Cycloadducts (7f/7g) Using in Situ Generated AgNPs. A mixture of activated dienophiles **5f/5g** (0.1 g, 1.0 equiv) and 2,3-dimethyl-1,3-butadiene, **6** (4.0 equiv), were mixed together in 10 mL of $\text{EtOH}:\text{H}_2\text{O}$ (1:1) solvent mixture in the presence of AgNPs (0.07 mmol). The reaction mixture was stirred at room temperature for 3 h. After completion of the reaction, the ethanol was removed under reduced pressure, and the remaining aqueous solution was extracted using pentane (2 \times 10 mL). The organic layer was dried over anhydrous Na_2SO_4 and distilled off to yield the desired product (7f). In case of reaction between **5g** and **6**, solid product (7g) was separated out after 3 h, filtered, and recrystallized using ethanol for 3 h. The aqueous layer containing AgNPs was used as such in the next catalytic reaction.

Compound 7f. (6,7-Dimethyl-3,4,4a,5,8,8a-hexahydro-2H-chromene): (Colorless liquid, 0.15 g in 78% yield). ^1H NMR (300 MHz, CDCl_3 , ppm) δ = 1.40–1.43 (m, 4H), 1.90 (s, 6H), 2.39–2.46 (m, 4H), 2.81–2.83 (m, 1H), 3.62 (t, 2H, J = 3.8 Hz), 4.19–4.24 (m, 1H). ^{13}C NMR (125 MHz, CDCl_3 , ppm) δ = 19.0, 25.2, 29.7, 30.7, 31.9, 63.8, 94.4, 112.6; ESI-MS mass spectrum of compound **7f** showed a parent ion peak, m/z = 205.0989 [$\text{M} + \text{K}$] $^+$. Elemental analysis: Calcd for $\text{C}_{11}\text{H}_{18}\text{O}$: C 79.46; H 10.91; O 9.62. Found: C 79.43; H 10.89; O 9.60.

Compound 7g.⁴⁰ (5,6-Dimethyl-3a,4,7,7a-tetrahydroisobenzofuran-1,3-dione): (0.12 g in 65% yield) ^1H NMR (300 MHz, CDCl_3 , ppm) δ = 1.72 (s, 6H), 2.28 (d, 2H, J = 5.7 Hz), 2.46 (d, 2H, J = 5.7 Hz), 3.35 (t, 2H, J = 4.2 Hz).

General Procedure for Synthesis of DA Cycloadducts (9a/9b/9c/9d/9e) Using in Situ Generated AgNPs. In a 25 mL round-bottom flask, quinones **8a/8b/8c/8d/8e** (0.1 g, 1.0 equiv) and 2,3-dimethyl-1,3-butadiene, **6** (4.0 equiv), were mixed in 10 mL of $\text{EtOH}:\text{H}_2\text{O}$ (1:1) solvent mixture in the presence of AgNPs (0.07 mmol). After stirring at room temperature for 4 h, the solid product (9a/9b/9c/9d/9e) separated which was removed by filtration and recrystallized with ethanol, and the remaining filtrate containing AgNPs was used as such in the next catalytic reaction.

For the synthesis of DA cycloadducts **9d** and **9e**, reactants (**8d** and **8e**) were synthesized by reported methods^{41,42} (PS37-S42, Supporting Information).

Compound 8d. (6-Bromoanthracene-1,4-dione): (dark green solid, 0.035 g in 45% yield). ^1H NMR (300 MHz, CDCl_3 , ppm) δ = 7.09 (s, 2H), 7.77 (d, 1H, J = 8.7 Hz), 7.94 (d, 1H, J = 8.7 Hz), 8.24 (s, 1H), 8.54 (s, 1H), 8.61 (s, 1H); ^{13}C NMR (125 MHz, CDCl_3 , ppm) δ = 124.3, 127.8, 128.8, 131.6, 132.2, 133.1, 135.8, 140.1, 140.1, 184.4; ESI-MS mass spectrum of compound **8d** showed a parent ion peak, m/z = 288.9859 [$\text{M} + \text{H}$] $^+$. Elemental analysis: Calcd for $\text{C}_{14}\text{H}_7\text{BrO}_2$: C 58.57; H 2.46; O 11.14. Found: C 58.55; H 2.45; O 11.12. M.P. = 240–242 °C.

Compound 8e. (6,7-Dibromoanthracene-1,4-dione): (yellowish-green solid, 0.03 g in 40% yield). ^1H NMR (300 MHz, CDCl_3 , ppm) δ = 7.11 (s, 2H), 8.38 (s, 2H), 8.53 (s, 2H); ^{13}C NMR (125 MHz, CDCl_3 , ppm) δ = 126.8, 127.7, 129.4, 134.2, 134.2, 140.1, 184.0; ESI-MS mass spectrum of compound **8e** showed a parent ion peak, m/z = 389.8685 [$\text{M} + \text{Na}$] $^+$.

Elemental analysis: Calcd for $C_{14}H_6Br_2O_2$: C 45.94; H 1.65; O 8.74. Found: C 45.92; H 1.63; O 8.73. M.P. = 245–247 °C.

Compound 9a.⁴³ (6,7-Dimethyltetrahydro-4a,5,8,8a-1,4-naphthoquinone): (0.15 g in 84% yield). ¹H NMR (300 MHz, $CDCl_3$, ppm) δ = 1.63 (s, 6H), 2.04–2.10 (m, 2H), 2.36–2.42 (m, 2H), 3.16–3.21 (m, 2H), 6.65 (s, 2H).

Compound 9b.⁴⁴ (1,4,4a,9a-Tetrahydro-2,3-dimethylantranthraquinone): (0.12 g in 81% yield). ¹H NMR (300 MHz, $CDCl_3$, ppm) δ = 1.64 (s, 6H), 2.11–2.17 (m, 2H), 2.43–2.45 (m, 2H), 3.35–3.38 (m, 2H), 7.73–7.76 (m, 2H), 8.03–8.06 (m, 2H).

Compound 9c.⁴⁵ 2,3-Dimethyl-1,4,4a,12a-tetrahydrotetracene-5,12-dione): (0.11 g in 80% yield). ¹H NMR (300 MHz, $CDCl_3$, ppm) δ = 1.66 (s, 6H), 2.15–2.21 (m, 2H), 2.47–2.54 (m, 2H), 3.39–3.43 (m, 2H), 7.66–7.69 (m, 2H), 8.05–8.08 (m, 2H), 8.60 (s, 2H).

Compound 9d. (8-Bromo-2,3-dimethyl-1,4,4a,12a-tetrahydrotetracene-5,12-dione): (green solid, 0.1 g in 76% yield). ¹H NMR (300 MHz, $CDCl_3$, ppm) δ = 1.66 (s, 6H), 2.14–2.21 (m, 2H), 2.46–2.53 (m, 2H), 3.39–3.43 (m, 2H), 7.74 (d, 1H, J = 8.7 Hz), 7.93 (d, 1H, J = 8.7 Hz), 8.23 (s, 1H), 8.50 (s, 1H), 8.57 (s, 1H); ¹³C NMR (125 MHz, $CDCl_3$, ppm) δ = 18.9, 30.7, 47.3, 123.6, 123.8, 125.8, 127.6, 128.7, 131.4, 131.9, 132.7, 136.3, 198.0; ESI-MS mass spectrum of compound 9d showed a parent ion peak, m/z = 370.0563 $[M + H]^+$. Elemental analysis: Calcd for $C_{20}H_{17}BrO_2$: C 65.05; H 4.64; O 8.67. Found: C 65.03; H 4.63; O 8.65. M.P. = 250–253 °C.

Compound 9e. (8,9-Dibromo-2,3-dimethyl-1,4,4a,12a-tetrahydrotetracene-5,12-dione): (brown solid, 0.09 g in 73% yield). ¹H NMR (300 MHz, $CDCl_3$, ppm) δ = 1.66 (s, 6H), 2.16–2.22 (m, 2H), 2.46–2.53 (m, 2H), 3.39–3.42 (m, 2H), 8.36 (s, 2H), 8.48 (s, 2H). ¹³C NMR (125 MHz, $CDCl_3$, ppm) δ = 18.9, 30.6, 47.3, 123.5, 126.3, 127.6, 131.4, 134.0, 134.6, 197.5; ESI-MS mass spectrum of compound 9e showed a parent ion peak, m/z = 487.4008 $[M + K]^+$. Elemental analysis: Calcd for $C_{20}H_{16}Br_2O_2$: C 53.60; H 3.60; O 7.14. Found: C 53.58; H 3.59; O 7.11. M.P. = 260–262 °C.

■ ASSOCIATED CONTENT

📄 Supporting Information

The Supporting Information is available free of charge on the ACS Publications website at DOI: 10.1021/acs.joc.5b02495.

Characterization data, optical properties of derivative 4, kinetic studies of catalytic reactions, NMR data of DA cycloadducts, and tables showing comparison of photocatalytic/catalytic activity of present system over other catalytic systems reported in the literature (PDF)

■ AUTHOR INFORMATION

✉ Corresponding Author

*E-mail: vanmanan@yahoo.co.in.

Notes

The authors declare no competing financial interest.

■ ACKNOWLEDGMENTS

V.B. is thankful to the Science and Engineering Research Board (SERB), New Delhi (ref no. EMR/2014/000149) for financial support. R.C. is thankful to UGC (New Delhi) for a Junior Research Fellowship (JRF). We are also thankful to UGC (New Delhi) for the “University with Potential for Excellence” (UPE) project.

■ REFERENCES

- (1) Kotha, S.; Chavan, A. S.; Goyal, D. *ACS Comb. Sci.* **2015**, *17*, 253.
- (2) Jiang, X.; Wang, R. *Chem. Rev.* **2013**, *113*, 5515.
- (3) *Cycloaddition Reactions in Organic Synthesis*; Kobayashi, S., Jorgensen, K. A., Eds.; Wiley-VCH: New York, 2002.
- (4) Pindur, U.; Lutz, G.; Otto, C. *Chem. Rev.* **1993**, *93*, 741.
- (5) Tenaglia, A.; Gaillard, S. *Org. Lett.* **2007**, *9*, 3607.
- (6) Hilt, G.; du Mesnil, F.-X. *Tetrahedron Lett.* **2000**, *41*, 6757.
- (7) Lautens, M.; Tam, W.; Lautens, J. C.; Edwards, L. G.; Crudden, C. M.; Smith, A. C. *J. Am. Chem. Soc.* **1995**, *117*, 6863.
- (8) Nawrat, C. C.; Palmer, L. I.; Blake, A. J.; Moody, C. J. *J. Org. Chem.* **2013**, *78*, 5587.
- (9) Han, Z. Y.; Chen, D. F.; Wang, Y. Y.; Guo, R.; Wang, P. S.; Wang, C.; Gong, L. Z. *J. Am. Chem. Soc.* **2012**, *134*, 6532.
- (10) Payette, J. N.; Yamamoto, H. *J. Am. Chem. Soc.* **2007**, *129*, 9536.
- (11) Ryu, D. H.; Zhou, G.; Corey, E. J. *J. Am. Chem. Soc.* **2004**, *126*, 4800.
- (12) Lin, S.; Padilla, C. E.; Ischay, M. A.; Yoon, T. P. *Tetrahedron Lett.* **2012**, *53*, 3073.
- (13) Lin, S.; Ischay, M. A.; Fry, C. G.; Yoon, T. P. *J. Am. Chem. Soc.* **2011**, *133*, 19350.
- (14) Hurlley, A. E.; Cismesia, M. A.; Ischay, M. A.; Yoon, T. P. *Tetrahedron* **2011**, *67*, 4442.
- (15) Cong, H.; Becker, C. F.; Elliott, S. J.; Grinstaff, M. W.; Porco, J. A., Jr. *J. Am. Chem. Soc.* **2010**, *132*, 7514.
- (16) Rycenga, M.; Cobley, C. M.; Zeng, J.; Li, W.; Moran, C. H.; Zhang, Q.; Qin, D.; Xia, Y. *Chem. Rev.* **2011**, *111*, 3669.
- (17) Kataria, M.; Pramanik, S.; Kaur, N.; Kumar, M.; Bhalla, V. *Green Chem.* **2015**, DOI: 10.1039/C5GC02337H.
- (18) Pramanik, S.; Bhalla, V.; Kumar, M. *ACS Appl. Mater. Interfaces* **2015**, *7*, 22786.
- (19) Kaur, S.; Bhalla, V.; Kumar, M. *Chem. Commun.* **2015**, *51*, 526.
- (20) Kaur, S.; Kumar, M.; Bhalla, V. *Chem. Commun.* **2015**, *51*, 4085.
- (21) Pramanik, S.; Bhalla, V.; Kumar, M. *Chem. Commun.* **2014**, *50*, 13533.
- (22) Sharma, K.; Singh, G.; Singh, G.; Kumar, M.; Bhalla, V. *RSC Adv.* **2015**, *5*, 25781.
- (23) Kundu, S.; Lau, S.; Liang, H. *J. Phys. Chem. C* **2009**, *113*, 5150.
- (24) Okamoto, T.; Bao, Z. *J. Am. Chem. Soc.* **2007**, *129*, 10308.
- (25) Liang, J.; Chen, Z.; Yin, J.; Yu, A. G.; Liu, S. H. *Chem. Commun.* **2013**, *49*, 3567.
- (26) Zhang, X.; Chi, Z.; Xu, B.; Chen, C.; Zhou, X.; Zhang, Y.; Liu, S.; Xu, J. *J. Mater. Chem.* **2012**, *22*, 18505.
- (27) Dong, S.; Li, Z.; Qin, J. *J. Phys. Chem. B* **2009**, *113*, 434.
- (28) Yang, Z.; Chi, Z.; Xu, B.; Li, H.; Zhang, X.; Li, X.; Liu, S.; Zhang, Y.; Xu, J. *J. Mater. Chem.* **2010**, *20*, 7352.
- (29) Jana, N. R.; Gearheart, L.; Murphy, C. J. *Chem. Mater.* **2001**, *13*, 2313.
- (30) Han, M. Y.; Quek, C. H.; Huang, W.; Chew, C. H.; Gan, L. M. *Chem. Mater.* **1999**, *11*, 1144.
- (31) Alahmad, A.; Eleoui, M.; Falah, A.; Alghoraibi, I. *Phys. Sci. Res. Int.* **2013**, *14*, 89.
- (32) Upert, G.; Bouillere, F.; Wennemers, H. *Angew. Chem., Int. Ed.* **2012**, *51*, 4231.
- (33) Lu, W.; Qin, X.; Li, H.; Asiri, A. M.; Al-Youbi; Abdulrahman, O.; Sun, X. *Part. Part. Syst. Character.* **2013**, *30*, 67.
- (34) Feng, J.; Zhang, P.; Wang, A.; Liao, Q.; Xi, J.-L.; Chen, J.-R. *New J. Chem.* **2012**, *36*, 148.
- (35) Kim, J.; Kang, S. W.; Kang, Y. S. *Colloids Surf., A* **2008**, *320*, 189.
- (36) Pramanik, S.; Bhalla, V.; Kumar, M. *ACS Appl. Mater. Interfaces* **2014**, *6*, 5930.
- (37) Hilt, G.; du Mesnil, F.-X. *Tetrahedron Lett.* **2000**, *41*, 6757.
- (38) Zheng, H.; Hall, D. G. *Tetrahedron Lett.* **2010**, *51*, 3561.
- (39) Falcicola, C. A.; Tissot-Croset, K.; Reyneri, H.; Alexakis, A. *Adv. Synth. Catal.* **2008**, *350*, 1090.
- (40) Li, J.; Xiong, Y.; Wu, Q.; Wang, S.; Gao, X.; Li, H. *Eur. J. Org. Chem.* **2012**, *31*, 6136.
- (41) Swartz, C. R.; Parkin, S. R.; Bullock, J. E.; Anthony, J. E.; Mayer, A. C.; Malliaras, G. G. *Org. Lett.* **2005**, *7*, 3163.

(42) Okamoto, T.; Senatore, M. L.; Ling, M.; Mallik, A. B.; Tang, M. L.; Bao, Z. *Adv. Mater.* **2007**, *19*, 3381.

(43) Naumann, S.; Unold, J.; Frey, W.; Buchmeiser, M. R. *Macromolecules* **2011**, *44*, 8380.

(44) Nishimoto, K.; Kim, S.; Kitano, Y.; Tada, M.; Chiba, K. *Org. Lett.* **2006**, *8*, 5545.

(45) Gupta, D. N.; Hodge, P.; Khan, N. *J. Chem. Soc., Perkin Trans. 1* **1981**, 689.